High Speed Laser Crystallization of Nanoparticle Ink for Thin Film Solar Cells at Room Temperature

Martin Y. Zhang and Gary J. Cheng*
Birck Nanotechnology Center and School of Industrial Engineering,
Purdue University, West Lafayette, IN 47906
email: gjcheng@purdue.edu

ABSTRACT

Cost effective and rapid thermal processing technique called direct pulsed laser crystallization (DPLC) is introduced to crystallize photovoltaic nanoparticle ink for thin film solar cell applications at room temperature and atmospheric pressure. DPLC improves the optical and electrical properties of the absorbent thin film by reducing internal defects of such as inter-crystal gaps and grain boundaries. CuInSe2 nanoparticle ink formed film was used as demonstration in current study, its film resistivity decreases by two orders of magnitude and hall mobility of charge carriers increases by two orders of magnitude as a result of DPLC. Band gap shrinkage (ΔEg) of CIS thin film after DPLC leads to broader acceptance of solar spectrum up to 100 nm. A typical increase of 7.9% (visible range) and 19.2% (near infrared range) in optical absorptance is obtained under optimal DPLC conditions.
Keywords: nanoscale superplastic nanoforming, pattering, metallic thin films, laser shock

Photoactive semiconductor materials used for thin film solar cells (TFSC), such as copper indium diselenide (CIS) and related material (CIGS), have been considered one of the most promising photovoltaic technologies with demonstrated high efficiency in both lab scale cells[1] (~19.9%) and large scale modules[2] (~13.4%). However, the conversion efficiency could be higher. In order to approach the theoretic limit, world-wide research and development (R&D) have been carried out for years to improve the quality of TFSC, especially on the absorbent layer. The most often seen obstacles are defects in the absorbent layer, such as grain boundaries, and inter-crystal gaps. Rapid thermal annealing (RTA) has been widely used to reduce internal defects because of its relatively low cost and uniform crystallization. However, RTA has some intrinsic problems, such as slow, high temperature, quasi-static temperature change leading to poor control of grain size, use of costly vacuum/inert gas systems. In addition, RTA is a non-selective heating process, not suitable for low melting point and large area substrates.

Cost effective and rapid thermal processing called direct pulsed laser crystallization (DPLC) is introduced in this study. DPLC has the following advantages: (1) *lower temperature*: compared with RTA operating at ~450 ^{o}C, DPLC operates at room temperature and because of use of CIS nanoink, the resulting temperature required is significantly lower than when bulk CIS is used due to size effects; smaller laser fluence is usually required as a result of stronger laser-nanoparticles interactions; (2) s*elective processing*: different materials absorb laser energy at different wavelength, such as CIS at visible region, while transparent conductive layer (e.g. aluminum-doped ZnO) absorbs laser at ultraviolet region. By selecting appropriate laser wavelength, DPLC selectively processes only the material that is intended to process and let other materials intact; (3) *better property*: the large crystal size and low defect density after multiple laser crystallization are important for better electrical properties since they will increase hall mobility of charged carriers and reduce electrical resistivity; (4) *higher speed*: DPLC is finished within 150 nanosecond (i.e. 30 pulses of 5 nanoseconds laser pulse) to produce high quality photovoltaics thin films. It is promising for commercialized scalable process if utilize high frequency (50-100 kHz) laser; (5) *energy save*: unique laser-nanoparticle interaction generates rapid temperature raising and decreasing, which makes high temperature controlling system unnecessary. Compared with existing methods that required deliberate temperature control and ambient gas systems, DPLC consumes much less energy during production.

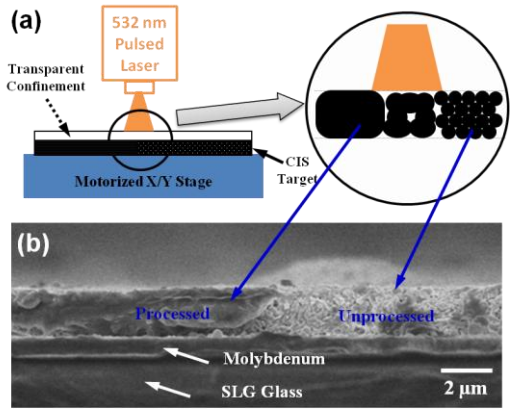

FIG. 1: (a) Methodology of low cost DPLC of CIS thin film. (b) Cross sectional FESEM images shows different morphology of CIS thin film before (right) and after (left) DPLC processing.

Copper indium diselenide (CIS) nanoparticle ink formed thin films are processed by DPLC at room temperature and atmospheric pressure to reduce internal defects, as seen in FIG. 1a. Continuum Surelite^{TM} Nd:YAG pulsed laser operated at 1064 nm and second harmonic

generation (532 nm) with 5 ns pulsed duration are used. The selected wavelength makes laser interacting with only CIS while letting other materials alone. Different laser fluence could be achieved by adjusting the power attenuator and focus lens to obtain different pulse energy and beam size. The target sample is placed at a PC-controlled motorized stage to enable x-y translation. CIS thin films are deposited on Molybdenum covered SLG. For Hall Effect and optical measurements, CIS is deposited directly on bare SLG substrates. Samples are then covered with a transparent glass on top (FIG. 1a) before being irradiated by laser pulses. Top confinement glass confines laser generated heat and pressure, and minimizes the oxidization during DPLC. More details on experiment could be found elsewhere.[3]

Hitachi® S4800 field emission scanning electron microscope (FESEM) is employed to determine both top and cross section morphologies of CIS films. Lambda® 950 spectrophotometer is used to measure film transmittance and absorptance spectra, and accordingly band gap is determined by plotting the absorbance squared versus energy, and extrapolating to zero. Properly calibrated Panalytical® MRD X'Pert Pro high resolution X-ray Diffraction (XRD) is utilized to identify the structural properties of CIS thin films. Hall Effect measurement consisting of MMR® MPS-50 power supply and H-50 Van der Pauw controller are used to measure film resistivity, hall mobility and carrier concentration of CIS thin films at room temperature.

Multiphysics modeling coupling electromagnetic (EM) with heat transfer (HT) module is employed to understand the laser and CIS nanoparticles interactions during DPLC. EM module is used to mimic how the laser (as a EM wave) interacts with CIS nanoparticles which ends up with resistive heating; HT transfer module then utilize resistive heating as the heat source to calculate the final temperature distribution in the system. More details could be found elsewhere. [4]

Experiments revealed that explosive crystallization initiated by laser induced rapid heating and cooling dominates the DPLC process. It involves three main phases (FIG. 2) in an optimal process (laser fluence = 24 mJ/cm^2). With the irradiation of first few (<10) laser pulses, loosed nanoparticles are densified and inter-particle voids are reduced as the laser induced pressure generated under the confinement media. Since laser penetration depth is usually in the scale of tens of nanometers, in phase 1, a very thin layer of CIS at the surface is altered, refer to the insert of FIG. 2b. When about 20 laser pulses are applied, CIS nanoparticles start to melt, however, at different rates due to uneven temperature distributions in the film. Neighbor molten CIS are merged together to reduce its total surface and strain energy. Melting and solidification induced crystallization penetrates deeper because higher effective thermal conductivity in the crystallized particles which conducts heat energy faster (less void defects and bigger in size[4]). After applying 30 laser pulses, surrounding CIS particles impinge to form larger crystals to further minimize total surface and strain energy. This process stops when the system reaches a thermodynamic equilibrium. As a result, original nanoparticles are all converted to crystallized large crystals as observed in FIG. 2d. It is worthy to note that when more than 30 laser pulses were delivered, porous structure started to form on top surface which is probably due to the ablation of CIS. The reason for ablation occurring only to grown crystals is because larger crystals have higher conductivities, and high laser absorption efficiency.[4-7] When irradiating laser at grown CIS crystals, ablation of CIS crystals occurs.

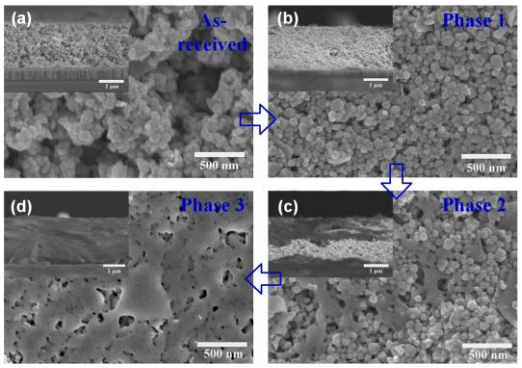

FIG. 2: Laser pulse number dependence of direct pulsed laser crystallization: (a) as-received, (b) 10 pulses, (c) 20 pulses, and (d) 30 pulses. Laser fluence (F) used was 24 mJ/cm^2. Cross section imaging for each case are inserted. The scale bar in inserts is 1 μm.

Applied laser fluence plays a significant role in DPLC. Optimal laser fluence (24 mJ/cm^2) would lead to smooth and packed CIS crystals where void defects are minimized (FIG. 3c). It is found that the laser fluence used in current study is much lower than prior reported studies[8], which is mainly attributed to the nanoscale size effect on enhancement on laser-nanoparticle interaction[4] and depression on melting point of nanoparticles. Laser fluence under threshold (e.g. 10 and 16 mJ/cm^2, FIG. 3a, and 3b) would lead to incomplete crystallization as supplied heat energy is inadequate. On the other hand, laser fluence obviously higher than optimal would lead to ablation to CIS which leads to damaged integrity and porosity in film structure (FIG. 3d).

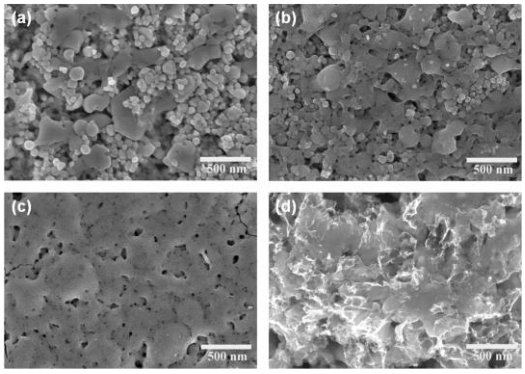

FIG. 3: Laser fluence dependence of direct pulsed laser crystallization: (a) 10, (b) 16, (c) 24 and (d) 34 mJ/cm^2. Laser pulse number (N) was 30.

Using small CIS nanoparticles in DPLC can effectively reduce the processing temperature and laser fluence. Multiphysics simulation found that optimal laser fluence is also dependent on CIS particle size since the temperature raise per unit laser fluence (ΔT) is strongly dependent on the size of CIS; the smaller the nanoparticles are, the larger then ΔT is. For CIS with diameter of 25, 50, 150, 300 and 600 nm, multiphysics model calculates that the corresponding ΔT is 34.1, 28.7, 24, 21.3 and 18.9 K/mJ·cm^{-2}, respectively. Knowing melting point for nanoparticles with certain size, the laser fluence used to crystallize CIS nanoparticles with diameter of 25, 50, 150, 300 and 600 nm is calculated to be 18.6, 23.3, 29.1, 32.9 and 37.2 mJ/cm^2, respectively. The nanoscale size effect on laser-nanoparticle interactions is responsible for this effect since smaller nanoparticles have stronger interactions with laser[4] thus resulting in higher temperature raise.

A comparison of XRD spectra before and after DPLC is shown in FIG. 4a. Before DPLC processing, major diffraction peaks (2-Theta) observed are at 26.65°, 44.22°, 52.39° which can be indexed to (112), (204)/(220), (116)/(312) of the crystal structure, respectively. Shifting of peaks is observed after DPLC, which indicates the introduction of film stress caused by DPLC. There is a 30% increase in the amplitude of (112) peak, which means there is a corresponding increase in crystal quality due to DPLC which probably due to increase in grain size and decrease internal defects. The increase of grain size is confirmed with Scherrer equation that it increases from 20 nm to 32 nm after DPLC (60% increase in size). The XRD spectra also indicate that the stoichiometry integrity of $CuInSe_2$ where no indication of thermal decomposition is found after DPLC processing.

The transmittance spectra of as-received and DPLC processed CIS films are measured directly and its absorptance spectra are calculated from Beer's law[9] (FIG. 4b). DPLC-processed samples show obvious increase in absorptance throughout the visible to near infrared region (500-1200 nm), while decrease between 400 and 500 nm. Between 500 and 800 nm, the average increase of optical absorptance is 7.85%. In the wavelength of 535 nm, there is a 5.2% increase in absorptance after DPLC treatment, this agrees with earlier studies.[4-7] In the near infrared (800 to 1200 nm) region, the DPLC-processed sample is at least 11.6% higher at 800 nm, 18.4% at 1000 nm, and 29.3% at 1200 nm in absorptance than the as-received sample. Overheated CIS thin film (DPLC-2 in FIG. 4b) displays worse optical properties compared with optimal DPLC and as-received samples, probably due to high density of porosity and inter-crystal voids as a result of laser ablation.

The band gap (E_g) of both as-received and DPLC-processed is determined to be 1.07 and 1.01 eV, respectively, see FIG. 4c. Both measured values are in good agreement with the reported value (1.04 eV) for bulk CIS.[10] However, small band gap shrinkage (~60 meV) is observed after DPLC treatment, which widens the acceptable range from 1158 to 1228 nm. Similar phenomena are observed by prior experimental results[11] and theoretical prediction, the B-M model that describes the relation between band gap shrinkage and carrier concentration.[12-14] Substituting values in the B-M model with measured carrier concentration density n = 1.493 x10^{18} cm^{-3} (see Table I), band gap shrinkage (ΔE_g) is then calculated to be 57.6 meV. This agrees well with the measured 60 meV from optical measurements. This is ascribed to the diffusion of copper combined with the fact that the electron effective mass of CIS is small, makes it degenerate at a relatively low concentration, which causes a shift in bandgap.[14]

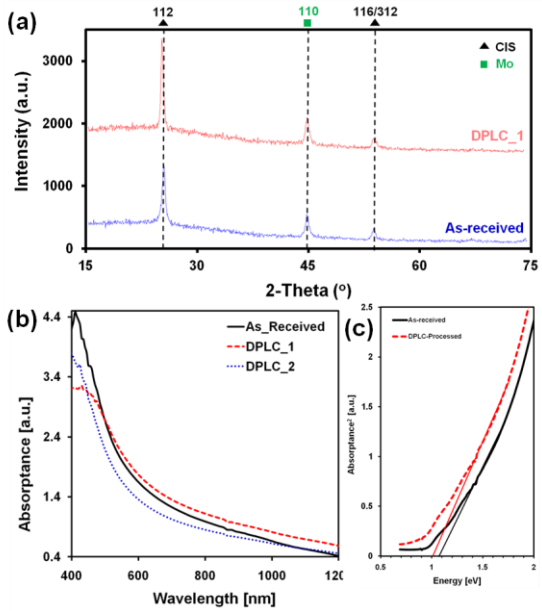

FIG. 4: (a) XRD spectra of as-received and DPLC processed CIS thin film. (b) Visible-near infrared absorptance spectra of as-received and DPLC processed CIS absorber materials. DPLC-1 stands for optimal and DPLC-2 for overheated DPLC. (c) The band gap (E_g) of the CIS is approximated using the direct band gap method (see Ref. 10).

Hall Effect measurements indicate that electrical resistivity decreases by two orders of magnitude, hall mobility increases by two orders of magnitude, and carrier concentration density slightly decreases after optimal DPLC processing. Both measured hall mobility and carrier concentration density are comparable to single phase CIS epitaxial layers that Newmann and co-workers[15] grown by single source evaporation at 780 K. Measured hall mobility is twice as high as what obtained in bulk single crystal CIS grown by Irie *et al*. at room temperature.[16] Measured carrier concentration density is one to two orders of magnitude higher than single crystal CIS thin film grown by Schroeder *et al*. at 1000 K[17], and three orders of magnitude higher than single crystals grown by Bridgman method at 1400 K.[18] It is worthy to note that overheated DPLC conditions would lead to worse electrical properties due to laser

ablation induced porosity that impedes movement of charged carriers (DPLC-2 in TABLE I).

TABLE I: Comparison of electrical resistivity, hall mobility and carrier concentration of as-received and DPLC treated CIS vs. prior literatures

AZO Films	Resistivity (Ωcm)	Hall Mobility (cm^2/vs)	Carrier Density (cm^{-3})
Irie *et al*.	~0.1	10	$\sim 1\times10^{16}$
Shaban *et al*.	0.148	956	$\sim 1.09\times10^{15}$
As-Received	15.162±0.026	0.266±0.091	$(1.681\pm0.599)\times10^{18}$
DPLC-1[a]	0.182±0.002	22.003±3.920	$(1.493\pm0.256)\times10^{18}$
DPLC-2[b]	25.883±0.067	0.162±0.004	$(1.487\pm0.042)\times10^{18}$

[a]: DPLC-1 under optimal processing conditions.
[b]: DPLC-2 under overheated processing conditions (ablation occurred).

To sum up, direct pulsed laser crystallization (DPLC) is developed in this study to improve optical and electrical properties of CIS thin film for thin film solar cell applications. Optimal DPLC processing (532 nm in wavelength, 5 ns in pulse duration, 24 mJ/cm^2 in laser fluence and 30 pulses) operated at room temperature and atmospheric pressure leads to properties as superior as single crystal CIS thin films at elevated temperatures. This is because nanosecond laser pulse generated local rapid heating and cooling processes significantly minimize internal defects, i.e. grain boundary density and inter-crystal gaps, in the microstructure of CIS particles. After optimal DPLC, an average increase of 7.9% and 19.2% in optical absorptance is obtained in the visible and near-infrared regions, respectively. Band gap of CIS slightly decreases by 60 meV which widens the solar spectrum absorption edge by 70 nm (from 1158-1228 nm). The film electrical resistivity drops by 2 orders of magnitude while the hall mobility increases by 2 orders of magnitude.

Reference

1. I. Repins, M. Contreras, Y. Romero, Y. Yan, M. Metzger, J. Li, S. Johnston, B. Egaas, C. DeHart, J. Scharf, B.E. McCandles, R. Noufi, IEEE Photovoltaics Specialists Conference Record, 33 (2008).
2. A. Luque, S. Hegedus (Ed.), in Handbook of Photovoltaic Science and Engineering, John Wiley, Chichester, England, 567 (2003).
3. G.J. Cheng, M.Y. Zhang, Y. Yang, High Speed Laser Crystallization of Particles of Photovoltaic Solar Cells. US Patent No. PRF 65614.P1.
4. M.Y. Zhang, G.J. Cheng, J. Appl. Phys. **108**, 113112 (2010).
5. T. Savage, A.M. Rao, Thermal Properties of Nanomaterials and Nanocomposites, in Thermal Conductivity: Theory, Properties, and Applications, (Ed: Tritt T. M., Plenum), New York, 261 (2003).
6. A. J. Kulkarni, M. Zhou, Appl. Phys. Lett. **88**, 141921 (2006).
7. A. J. Kulkarni, M. Zhou, F. J. Ke, Nanotechnology **16**, 2749 (2005).
8. S.Park, B.L. Clark, D.A. Keszler, J.P. Bender, J.F. Wager, T.A. Reynolds, Science **287**, 65 (2002).
9. G.W.F. Drake (Ed.), Springer Handbook of Atomic, Molecular, and Optical Physics, Vol 1, Second Edition, Springer, Germany, 1000 (2006).
10. Q. Guo, S.J. Kim, M. Kar, W. N. Shafarman, R. W. Birkmire, E. A. Stach, R. Agrawal, H. W. Hillhouse, Nano Lett. **8**, 2982 (2008).
11. S. E. Aw, H. S. Tan, C. K. Ong, J. Phys.: Condens. Matter. **3**, 8213 (1991).
12. E. Burstein, Phys. Rev. **93**, 632 (1954).
13. T.S. Moss, Proc. Phys. Soc. (London) **B67**, 775 (1954).
14. C. Rincon, C.S. Perez, Solid State Commun. **50**, 899 (1984).
15. H. Newmann, E. Nowak, B. Schumann, G. Kuhn, Thin Solid Films **74**, 197 (1980).
16. T. Irie, S. Endo, S. Kimura, Jpn. J. Appl. Phys. **18**, 1303 (1979).
17. D.J. Schroeder, T.L. Hernandez, G.D. Berry, A.A. Rockett, J. Appl. Phys. **83**, 1519 (1998).
18. H.T. Shaban, M. Mobarak, M.M. Nassary, Physica B **389**, 351 (2007).